THE UNEXPECTED $^{187}Os/^{188}Os$ RESPONSE TO THE MID-CENOMANIAN EVENT: AN INVESTIGATION IN THE IONA-1 CORE

Liam Lauckner

APPROVED:

Dr. Alan Brandon

Dr. Qi Fu

Dr. Shuhab Khan

Dr. Dan Wells, Dean

College of Natural Sciences and Mathematics

THE UNEXPECTED $^{187}Os/^{188}Os$ RESPONSE TO THE MID-CENOMANIAN EVENT: AN INVESTIGATION IN THE IONA-1 CORE

A Senior Honors Thesis Presented to

the Faculty of the Department of Earth and Atmospheric Sciences

University of Houston

In Partial Fulfillment

of the Requirements for the Degree

Bachelor of Science

By

Liam Lauckner

December 2018

ABSTRACT

The emplacement of either the Caribbean Large Igneous Province (CLIP) or High Arctic Large Igneous Province (HALIP) is implicated in the triggering of the Cenomanian-Turonian Ocean Anoxic Event 2 (OAE-2; ca 94 - 95 Ma). Evidence for a similar initiation mechanism for the Mid-Cenomanian Event (MCE; ca 96.5 Ma), a precursor to OAE-2 during which comparable environmental conditions persisted, is contradictory or absent. In this study, a reconstruction of mid-Cenomanian seawater $^{187}Os/^{188}Os$ from the Iona-1 core, SW Texas, the first for the Cretaceous Western Interior Seaway, tests the role of LIP activity in triggering the MCE. The absence of a prolonged unradiogenic Os-isotope excursion (low $^{187}Os/^{188}Os$) during the MCE interval argues against CLIP involvement in the event's initiation. Instead, the coincidence of a muted unradiogenic Os-isotope excursion and elevated Hg concentrations with published ^{40}Ar-^{39}Ar ages of 96.4 Ma of basalts from Ellesmere Island, Canada, suggests HALIP-related volcanic activity may have precipitated the MCE. In addition, the correlation of a pronounced radiogenic Os-isotope excursion (high $^{187}Os/^{188}Os$) between Iona-1 and previous measurements from the English Chalk, Eastbourne, England, provides evidence for elevated pCO_2, an accelerated global hydrologic cycle and increased continental weathering rates – conditions known to exist during OAE-2 but previously only postulated for the MCE.

CONTENTS

FIGURES

TABLES

1. INTRODUCTION

1.1 Ocean Anoxic Events: The Mid-Cenomanian Event and Ocean Anoxic Event 2

Periods of extensive marine anoxia and disruption of the global carbon cycle, termed ocean anoxic events (OAEs) by Schlanger and Jenkyns (1976), interspersed the greenhouse world of the Cretaceous. Although the causes and effects of no two OAEs are identical, the progressions of most OAEs are comparable (see Jenkyns, 2010). Because of their proximity in time and associated development of anoxia, multiple workers have drawn comparisons between the Mid-Cenomanian Event (MCE; ca 96.5 Ma) and Ocean Anoxic Event 2 (OAE-2; ca 94 – 95 Ma) (Hardas et al., 2012; Zheng et al., 2016; Scaife et al., 2017; Beil et al., 2018), with some going so far as to label the MCE a "precursor" to OAE-2 (Coccioni and Galeotti, 2003). However, in contrast to OAE-2, for which numerous studies detail a comprehensive, unified chronology, the few existing investigations of the MCE paint an equivocal picture of its triggering (Zheng et al., 2016; Scaife et al., 2017) and progression (Coccioni and Galeotti, 2003; Moriya et al., 2007; Friedrich et al., 2009; Giraud et al., 2013; Andrieu et al., 2015). A need therefore exists to elucidate the initiation and development of the MCE, and to untangle the connectedness of the two carbon cycle perturbations.

Exhaustive geochemical, sedimentological and paleontological studies of Cenomanian-Turonian strata corroborate a comprehensive chronology for Ocean Anoxic Event 2. Multiple independent geochemical proxies suggest the onset of OAE-2 was preceded by the emplacement of either the Caribbean Large Igneous Province (CLIP;

Snow et al., 2005; Turgeon and Creaser, 2008; Du Vivier et al., 2014) or the High Artic Large Igneous Province (HALIP) (figure 1; Eldrett et al., 2014; Scaife et al., 2017). An associated increase in atmospheric pCO_2 is hypothesized to have raised atmospheric temperatures and accelerated the global hydrological cycle, thereby increasing continental weathering rates and, ultimately, the flux of nutrients to the oceans (Blätter et al., 2011; Wagner et al., 2013). Subsequently, these nutrients, particularly phosphorus, drove the increase in primary marine productivity that produced the anoxia of Ocean Anoxic Event 2. This narrative is complicated, however, by the recognition of 1.5 million years of intermittently anoxic conditions in portions of the Atlantic Basin prior to the onset of OAE-2, which began with the onset of the Mid-Cenomanian Event (MCE) (Coccioni and Galeotti, 2003).

Like OAE-2, the MCE is a globally-recognized $\delta^{13}C$ excursion (Paul et al., 1994; Mitchell et al., 1996, Coccioni and Galeotti, 2003; Voigt et al., 2004; Gale et al., 2008; Beil et al., 2018). However, anoxic conditions and extensive organic matter preservation were less pervasive than during OAE-2, with black shale deposition occurring in fewer localities (Coccioni and Galeotti, 2003; Friedrich et al., 2009; Minisini et al., 2008). Likewise, the only report of increased weathering rates during the MCE comes from an investigation of clay mineral assemblages in the Aquitaine Basin, France (Giraud et al., 2013). The evidence for a LIP triggering of the MCE is similarly muddled. A reconstruction of seawater εNd (Zheng et al., 2016) found no support for submarine volcanic activity during the event. Conversely, though an investigation of Hg concentrations in MCE-age strata concluded a LIP was active during the event, peak enrichments in Hg, and therefore LIP activity, occurred in the event's second half, not at its onset (Scaife et al., 2017).

1.2 The ^{187}Re-^{187}Os System and Application to Ocean Anoxic Events

The ^{187}Re-^{187}Os system is routinely examined in marine shales to investigate past environmental perturbations, such as OAEs (Cohen, 2004). Os exists in the earth's crust in two distinct reservoirs, both of which are characterized by disparate $^{187}Os/^{188}Os$ signatures. The in situ decay of ^{187}Re enriches the continental crust in ^{187}Os relative to ^{188}Os, with typical crustal $^{187}Os/^{188}Os$ values rising above 1. In contrast, mantle-derived basaltic rocks, which are depleted in Re, show $^{187}Os/^{188}Os$ ratios of ~0.14. The erosion and chemical weathering of these two sources impart seawater with their corresponding $^{187}Os/^{188}Os$ values (Peucker-Ehrenbrink, 2000). Through geologic time, the $^{187}Os/^{188}Os$ value of the oceans has varied (Peucker-Ehrenbrink and Ravizza, 2012), with heterogeneities existing on scales of as little as a few hundred kilometers (Rooney et al., 2016; Coe et al., 2017). No detectable mass-dependent isotopic fractionation occurs when Os is removed from seawater and absorbed onto organic matter on the seafloor. Therefore, it is possible to reconstruct the $^{187}Os/^{188}Os$ of ancient seawater by subtracting the in situ formation of ^{187}Os by ^{187}Re decay from modern $^{187}Os/^{188}Os$ values of marine rocks. This reconstructed seawater $^{187}Os/^{188}Os$ is termed Os_i. Because Os has a short ocean residence time of 10 – 40 k.y. (Peucker-Ehrenbrink, 2000) or less (Rooney et al., 2016), the Os_i proxy can track the rapid fluctuations of weathering patterns, as occurred during ocean anoxic events that spanned 100 to 500 k.y. In addition, Os_i is known to respond to fluxes in Os input during glacial-interglacial cycles and extraterrestrial impact events.

An Atlantic-wide excursion of Os_i to highly unradiogenic values of ~0.2 prior to the onset of OAE-2 is the most compelling evidence for a LIP's role in triggering that event and highlights the application of the ^{187}Re-^{187}Os system for examining the balance between mantle and continental inputs to the global ocean (Turgeon and Creaser, 2008; Du Vivier et al., 2014). With the exception of a preliminary report from the English Chalk (Jarvis et al. 2017, 2018), no ^{187}Os/^{188}Os data is available on MCE strata. In this study, an Os_i record of the MCE for the KWIS, from samples from the Iona-1 Core (figure 1), is presented to test for LIP activity during the mid-Cenomanian and to draw comparisons between the environmental conditions that existed during both the MCE and OAE-2. In addition, the distributions of the platinum group elements (PGEs; Os, Ir, Ru, Pt and Pd) and Re in the Iona-1 core are reported and analyzed to test the validity of the Iona-1 Os_i reconstruction.

Although the discussion largely considers a LIP control on the reconstructed Os-isotope, the impact of a purported glaciation event during the mid-Cenomanian is also considered. However, the Iona-1 Os_i data are largely interpreted as compelling evidence for the role of the HALIP in triggering the MCE. Because of the proximity of the Iona-1 core to the CLIP (figure1 1), the lack of a mantle-like unradiogenic Os_i excursion during the MCE in Iona-1 argues against CLIP volcanism prior to or during the MCE. Instead, an extremely radiogenic Os_i excursion at the MCE's onset, which is consistent with elevated pCO_2 and therefore weathering rates because of LIP activity – precedes a muted unradiogenic Os_i excursion, the age of which perfectly correlated with those of known HALIP basalts.

2. MATERIALS AND METHODS

2.1 The Iona-1 Core

The samples used in this study are Cenomanian organic-rich marls and carbonates from the Lower Eagle Ford Formation, Maverick Basin, SW Texas, which were recovered by the Iona-1 core (29°13.51'N, 100°44.49'W; Figure 1) in 2012. Previous efforts by Eldrett et al. (2014, 2015a, 2015b, and 2017) and Minisini et al. (2018) synthesized descriptions of the core's stratigraphy, biostratigraphy, and trace metal and $\delta^{13}C$ chemostratigraphy to interpret the Eagle Ford's depositional history and the impact of the MCE and OAE-2 on the Southern Cretaceous Western Interior Seaway. In summary, Iona-1 Eagle Ford strata were deposited in a distal, sediment-starved foreland basin at a paleowater depth of ~ 50-200 m (Eldrett et al., 2014). The MCE is identified in a 5-m-long section of core by a characteristic double-peak $\delta^{13}C$ excursion (Paul et al., 1994) and a spike in organic matter content (Minisini et al., 2018). During the MCE, sea-level rose significantly and marine primary productivity reached a relative maximum (Minisini et al., 2018). Persistent anoxia in the KWIS during the MCE is suggested by a lack of bioturbation (Minisini et al., 2018).

2.2 Os Extraction and Measurement Procedures

Osmium was extracted from the Iona-1 samples by following standard procedures and then measured via isotope-dilution thermal ionization mass spectrometry. Before being powdered in a ceramic mortar and pestle, the surfaces of 14 Iona-1 core samples were cleaned using a carborundum block to remove potential contamination from previous contact with metal implements. Approximately 0.4 g of powder per sample were spiked in ^{99}Ru, ^{185}Re, ^{190}Os, ^{191}Ir, ^{194}Pt and ^{105}Pd (Shale Spike #2 and UMD Dil. Sp. C PGE) for isotope dilution, and then dissolved in 3 mL HCL and 6 mL HNO_3 in sealed carius tubes at 240 ^{0}C for 48-72 hours. After digestion, the carius tubes were frozen and unsealed, and the osmium was extracted from the contents using the chloroform extraction and hydrogen bromide back extraction techniques of Cohen and Waters (1996).

Following the above, the remaining chloroform phase was set aside for later Re and PGE purification and extraction. The osmium was then purified during microdistillation using CrO_3 in H_2SO_4 (Birck et al., 1997) Next, the osmium was loaded onto baked Pt filaments in HBr, coated with a $Ba(OH)_2$ activator solution, and measured as OsO^-_3 using a Thermofisher Triton Plus thermal ionization mass spectrometer in negative ion mode at the University of Houston. Finally, the raw Os-isotope measurements were corrected for spike input, oxygen-isotope interference, and instrumental mass fractionation during measurement to produce the raw $^{187}Os/^{188}Os$ values reported in figure 3.

2.3 Re and Platinum Group Element Extraction Procedures

Rhenium and the platinum group elements were separated by column chromatography before measurement. After being converted to a chloride phase, the Re and PGE aliquots were subjected to cation and anion chromatography. The PGE and Re fractions were then dissolved in HNO_3. An Agilent 8900 QQQ ICP-MS at the University of Houston was used to measure the PGEs and Re.

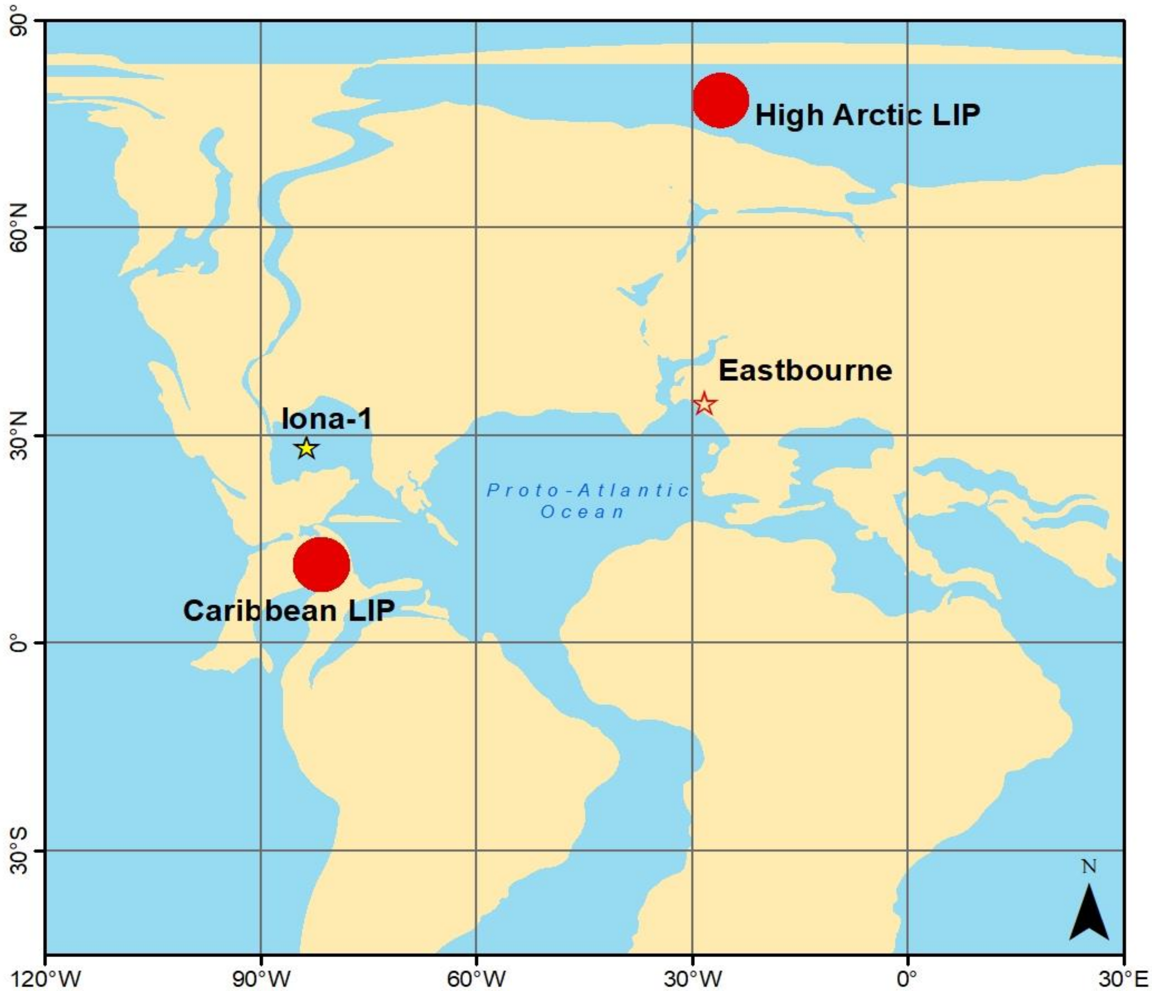

Figure 1: Map showing a paleogeographic reconstruction of the Proto-Atlantic Ocean and surroundings ca 96.5 Ma. The approximate locations of the Caribbean Large Igneous Province, High Arctic Large Igneous Province, Iona-1 core and Eastbourne section are indicated. (map modified from http://www.odsn.de/odsn/services/paleomap/paleomap.html)

3. RESULTS

3.1 Overview

In figure 2, Os_i values are plotted against $\delta^{13}C_{organic}$ (Eldrett et al., 2014), which defines the extent of the MCE (grey shading). The raw $^{187}Re/^{188}Os$ and $^{187}Os/^{188}Os$ measurements from which the Os_i data were calculated are shown in table 1, along with their 2σ uncertainties. In figure 3, PGE and Re distributions are given normalized to primitive upper mantle (PUM; Becker et al., 2006) and compared to typical upper continental crust values (Chen et al., 2016). Table 2 reports the PGE and Re parts-per-billion abundances and PUM normalizations.

3.2 Os_i Reconstruction

On the basis of comparison to the MCE $\delta^{13}C$ excursion, the Os_i record in the Iona-1 core is divided into 4 segments (figure 2). Before the onset of the MCE, in segment A, Os_i remained steady between 0.9 and 1.0, in good agreement with previous estimates of pre-OAE2 Os_i background values for the KWIS (Figure 2; Turgeon and Creaser, 2008; Du Vivier et al., 2014). In segment B, from the beginning of the positive $\delta^{13}C$ excursion that defines the onset of the MCE at 96.53 Ma, a rise in Os_i to a highly radiogenic maximum of 1.26 at 96.48 Ma coincides with the positive double-peak $\delta^{13}C$ maximum of the MCE (Paul et al., 1994). Thereafter, Os_i falls rapidly, reaching a mildly unradiogenic minimum of 0.65 at 96.4 Ma late in the MCE during segment C. In segment D, following the cessation of the MCE at 96.38 Ma, Os_i returned to background values of 0.9 to 1.0

3.3 Platinum Group Element Data

Re and PGE abundances are reported for all samples. No chemostratigraphic patterns are discernable for the PGEs. However, their Primitive Upper Mantle (PUM)-normalized distribution patterns are typical for upper continental crust sedimentary rocks (figure 3; Becker et al., 2006; Chen et al., 2016). Regardless, because of the paucity of investigations into the paleoenvironmental significance of PGEs (e.g. Sawlowicz, 1993), no further interpretations of their importance were made.

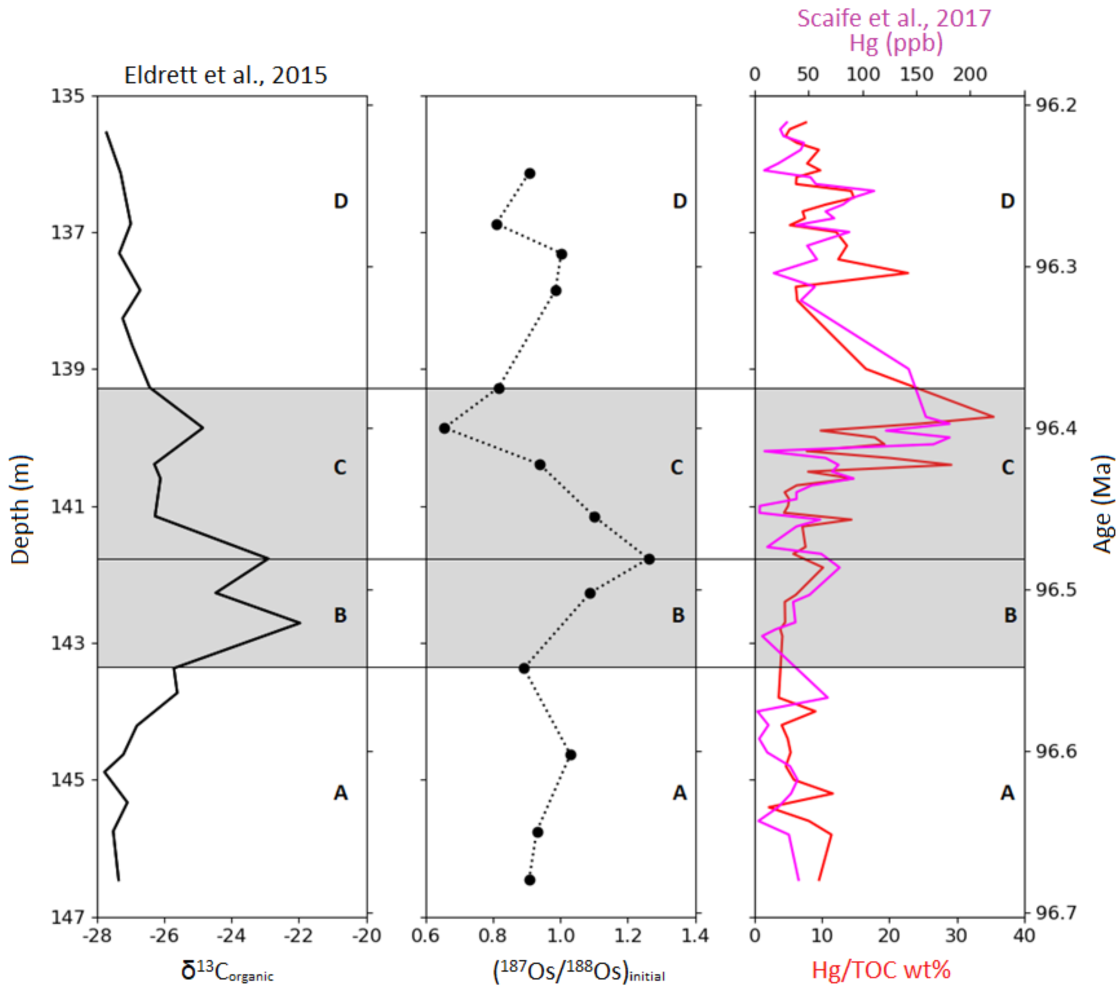

Figure 2: Plot showing $\delta^{13}C_{organic}$ (Eldrett et al., 2014), Os_I and Hg data (Scaife et al., 2017) for the Iona-1. The grey shading indicates the $\delta^{13}C$ excursion that defines the extent of the Mid-Cenomanian Event. The plot is divided into 4 segments: A, B, C and D. See text for discussion.

Table 1: Raw $^{187}Re/^{187}Os$ and $^{187}Os/^{188}Os$ measurements are shown, along with their corresponding 2σ uncertainties. Calculated Os_i values are also reported.

Sample Depth (m)	Sample Age (Ma)	$^{187}Re/^{188}Os$ (measured)	2σ $^{187}Re/188Os$	$^{187}Os/^{188}Os$ (measured)	2σ $^{187}Os/^{188}Os$ (measured)	$^{187}Os/^{188}Os$ (initial)	2σ $^{187}Os/^{188}Os$ (initial)
136.14	96.19	2555.16	20.184	5.005	0.049	0.907	0.016
136.88	96.23	2287.47	16.213	4.481	0.028	0.810	0.002
137.31	96.25	2400.81	22.763	4.856	0.037	1.003	0.001
137.85	96.28	2775.43	30.507	5.441	0.087	0.986	0.038
139.27	96.36	2017.01	22.544	4.058	0.040	0.817	0.004
139.86	96.39	1878.04	14.236	3.675	0.031	0.657	0.008
140.39	96.42	2124.95	13.822	4.355	0.013	0.939	0.009
141.15	96.45	2470.70	16.053	5.073	0.018	1.100	0.008
141.77	96.48	2453.43	36.441	5.208	0.073	1.262	0.015
142.27	96.50	2446.58	17.362	5.025	0.030	1.088	0.002
143.37	96.56	1962.16	12.746	4.051	0.014	0.892	0.007
144.63	96.62	2674.54	21.783	5.339	0.054	1.030	0.019
145.75	96.67	2975.25	166.013	5.726	0.096	0.930	0.172
146.46	96.70	3330.07	31.566	6.277	0.082	0.907	0.031

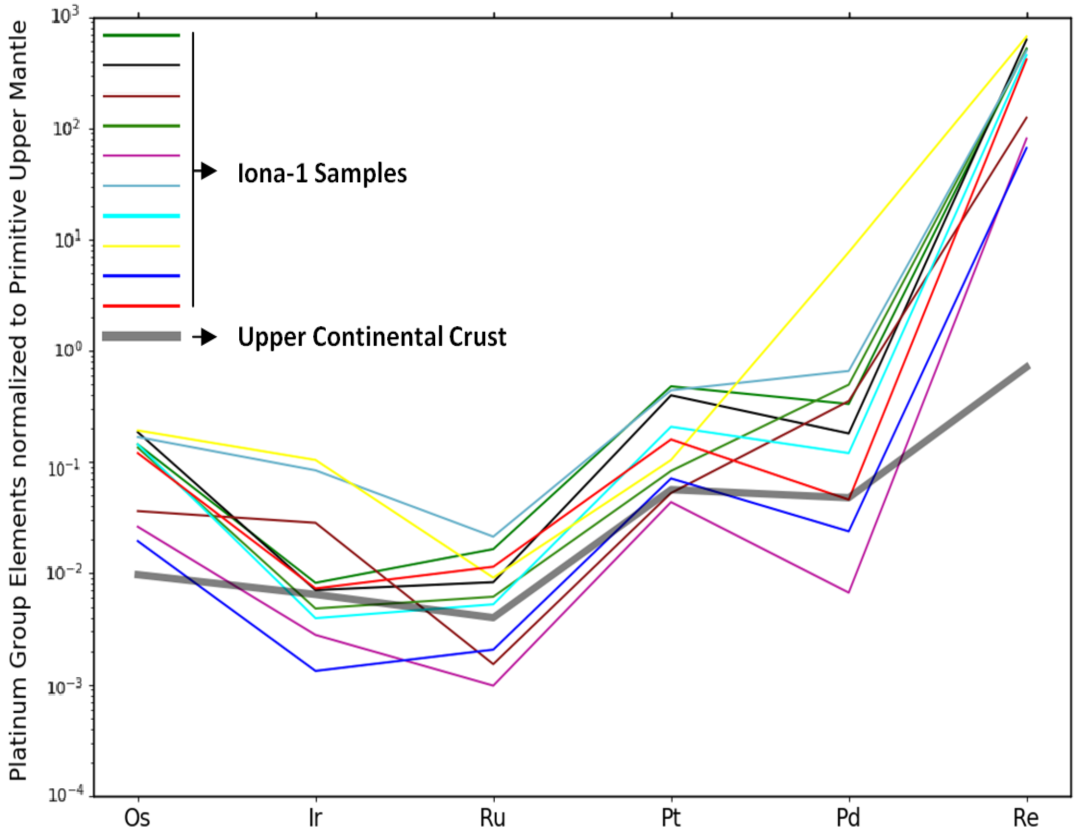

Figure 3: The distributions of platinum group element and rhenium abundances, normalized to primitive upper mantle (Becker et al., 2006), are compared to an average upper continental crustal value (Chen et al., 2016).

Table 2: In the first table, Iona-1 platinum group element and rhenium abundances are reported as parts-per-billion concentrations. The second table displays the PGE + Re values after normalization to primitive upper mantle (Becker et al., 2006).

Sample Depth (m)	Sample Age (Ma)	Os (ppb)	Ir (ppb)	Ru (ppb)	Pt (ppb)	Pd (ppb)	Re (ppb)
136.14	96.19	0.563297	0.027975	0.115713	3.64866	2.364775	114.7299
136.88	96.23	0.724723	0.024075	0.058377	3.030052	1.28561	137.9139
137.31	96.25	0.14158	0.09685	0.010705	0.401211	2.515035	27.42068
137.85	96.28	0.527545	0.016437	0.043214	0.633892	3.52824	112.791
139.27	96.36	0.102395	0.009514	0.006863	0.332421	0.047683	17.80829
139.86	96.39	0.65596	0.286992	0.149767	3.362254	4.687422	109.8586
140.39	96.42	0.561758	0.013448	0.036909	1.580831	0.855933	100.3588
141.15	96.45	0.751218	0.355624	0.064163	0.794505	54.79662	147.152
141.77	96.48	0.076081	0.004519	0.014449	0.542473	0.169469	14.64198
142.27	96.5	0.470136	0.024902	0.080356	1.215573	0.32677	91.54293
143.37	96.56	0.752955	0.005548	0.058618	2.749067	0.849743	127.4635
144.63	96.62	0.793667	0.078502	0.06202	2.046675	-0.00966	158.727
145.75	96.67	0.853547	0.038117	0.04924	1.304826	-0.02146	183.5869
146.46	96.7	1.038082	-0.01018	-0.01181	0.17262	0.121009	250.1981

Sample Depth (m)	Sample Age (Ma)	Os UCC-normalized	Ir UCC-normalized	Ru UCC-normalized	Pt UCC-normalized	Pd UCC-normalized	Re UCC-normalized
136.14	96.19	0.001122	6.3E-05	0.000178	0.004212	0.004162	4.617063
136.88	96.23	0.001444	5.42E-05	8.99E-05	0.003498	0.002263	5.550052
137.31	96.25	0.000282	0.000218	1.65E-05	0.000463	0.004426	1.103487
137.85	96.28	0.001051	3.7E-05	6.65E-05	0.000732	0.00621	4.539035
139.27	96.36	0.000204	2.14E-05	1.06E-05	0.000384	8.39E-05	0.716657
139.86	96.39	0.001307	0.000646	0.000231	0.003881	0.00825	4.421028
140.39	96.42	0.001119	3.03E-05	5.68E-05	0.001825	0.001506	4.038729
141.15	96.45	0.001496	0.000801	9.88E-05	0.000917	0.096439	5.92182
141.77	96.48	0.000152	1.02E-05	2.22E-05	0.000626	0.000298	0.589236
142.27	96.5	0.000937	5.61E-05	0.000124	0.001403	0.000575	3.683952
143.37	96.56	0.0015	1.25E-05	9.02E-05	0.003173	0.001495	5.129501
144.63	96.62	0.001581	0.000177	9.55E-05	0.002363	-1.7E-05	6.633034
145.75	96.67	0.0017	8.59E-05	7.58E-05	0.001506	-3.8E-05	7.703744
146.46	96.7	0.002068	-2.3E-05	-1.8E-05	0.000199	0.000213	10.06869

4. DISCUSSION

4. 1 Validity of the Os_i Reconstruction

4.1.1 Os_i Reconstruction Integrity

Reconstructions of seawater $^{187}Os/^{188}Os$ from marine shales can be invalidated if their Re-Os isotope systematics have been disturbed by post-depositional processes (Peucker-Ehrenbrink and Hannigan, 2000). For example, the oxidation of organic matter in a shale by weathering processes in exposed outcrops is known to free substantial fractions of both Re (~99%) and Os (~40%), including the fractions hosted in the organic matter (Jaffe et al., 2002). Although core samples are inherently less susceptible to alteration by surficial weathering processes (Peucker-Ehrenbrink and Hannigan, 2000), their Re-Os systems can be altered by diagenetic processes (Georgiev et al., 2012). Because the MCE-age core samples are beyond the reach of surface processes (> 120 m core depth), their Re-Os isotope systematics are likely to have remained closed since deposition. The distribution patterns of Re and the PGEs (figure 3) confirm this assumption. This is because oxidative alteration tends to decrease the concentrations of all these elements, especially Re and Os (Peucker-Ehrenbrink and Hannigan, 2000). The samples studied here from the Iona-1 core have significant enrichments in Os and Re relative to upper continental crust (Chen et al., 2016) and confirm that no discernable loss of either element has occurred. Therefore, the calculated Os_i values reflect ancient seawater $^{187}Os/^{188}Os$. An earlier Os-isotope study of OAE-2 in Iona-1 by Wright (2015) similarly encountered few or no altered samples. Additionally, the firm connection between the Southern KWIS and the Atlantic Ocean during the MCE (Minisini et al., 2018) means the reconstructed Os_i values reflect the $^{187}Os/^{188}Os$ of the ancient ocean, not an isolated basin.

4.1.2 Comparisons to the Eastbourne Section

The Os_i reconstruction is corroborated by unpublished Os_i data for the MCE from the English Chalk, Eastbourne, UK. Jarvis et al. (2017, 2018) report a pre-MCE Os_I range of 0.8 – 0.9 that is comparable to that of segment A in Iona-1 of 0.9 – 1.0 (figure 2). Moreover, both the radiogenic and unradiogenic excursions recorded in Iona-1 in segments B and C are observed in the English Chalk, with Os_i values of 1.2 and 0.2, respectively. The magnitude of the unradiogenic minimum in NW Europe is substantially greater than that seen in the KWIS, in line with the OAE-2 unradiogenic excursion of 0.2 found by Turgeon and Creaser (2008). Post-MCE Os_i values are not given by Jarvis et al. (2017, 2018). The excellent agreement of the results from the MCE from Iona-1 with those from the Eastbourne section is consistent with a scenario in which the Iona-1 Os_i data represent the global ocean.

4.2 The Mid-Cenomanian Glaciation Hypothesis

The Iona-1 Os_i dataset presented hare can be used to test the Mid-Cenomanian Glaciation Hypothesis. On the basis of apparently coeval sea-level fluctuations in the North Atlantic at ODP Site 856 and the Russian platform, and substantial carbonate $\delta^{18}O$ excursions indicative of cold temperatures (Stoll and Schrag, 2000), Miller et al. (2003, 2005) proposed the existence of glacioeustatic oscillations controlled by ephemeral

Antarctic glaciations during the mid-Cenomanian. Although later challenged by contradictory $\delta^{18}O$ records (Moriya et al., 2007; Ando et al., 2009), the theory continues to be countenanced (i.e. Beil et al., 2018). Despite the purported Antarctic glaciation's limited size and duration (Miller et al., 2003), Os_i may still track its impact on weathering rates, sea-level and climate.

If continental weathering rates fluctuated during the proposed mid-Cenomanian glacial-interglacial cycle, as during other glacial periods, a reduction(s) in the input of radiogenic Os from the continents to the oceans should be apparent in the Os_i reconstruction (figure 2). Glacial periods, during which sea-level is low and weathering rates are reduced, are known to correlate with decreased Os_i (Oxburgh, 1998; Williams and Turekain, 2004). In segment C of the Iona-1 Os_i data (figure 2) and in the English Chalk data, a substantial decrease in Os_i is observed, consistent with a marked reduction in radiogenic Os input from the continents to the global ocean. However, multiple lines of reasoning argue against a glacioeustatic origin for this excursion. A reconstruction of Cenomanian sea-level change (Gale et al., 2008) shows that a sea-level minimum in NW Europe occurred early in the MCE, when Os_i was highly radiogenic during segment B, not during the later portions of the event. In the KWIS, sea-level rose throughout the MCE interval (Minisini et al., 2018).

In either case, the Os_i minimum does not correspond with a global decline in sea-level, as is expected for glacial periods. Even if sea-level did not fluctuate in response to the hypothetical glaciation, associated temperature and climate variations could have instead driven Os_i changes by the varying continental weathering rates. Reconstructions of ocean temperatures from foraminifera $\delta^{18}O$ (Gale et al., 2002; Voigt et al., 2004) show a marked ocean temperature decrease during the MCE in the North Atlantic, during which weathering rates would be expected to decrease. However, this temperature minimum again corresponds with the radiogenic Os_i interval of segment B, not the unradiogenic minimum seen in segment C. Moreover, recent higher-resolution $\delta^{18}O$ benthic and planktonic foraminifera temperature reconstructions from Demerara Rise do not show these minimums at all (Moriya et al., 2007; Ando et al., 2009). Additionally, an investigation of clay assemblages from the Aquitaine Basin, France, indicates the MCE B segment was instead characterized by elevated temperatures and humidity (Giraud et al., 2013), not cooling.

Together, these lines of evidence do not support a glaciation-related reduction in temperature and consequently weathering rates during the MCE. Finally, the extremely radiogenic $^{187}Os/^{188}Os$ values documented in both segment B of Iona-1 and the Eastbourne reconstruction (Jarvis et al. 2017, 2018), which likely represent *increased* weathering rates, cannot be explained in the context of a mid-Cenomanian glaciation. Though known glacial-interglacial periods are characterized by oscillations between radiogenic and unradiogenic seawater $^{187}Os/^{188}Os$ (Oxburgh, 1998), a substantial radiogenic excursion above background Os_i is irreconcilable with the Mid-Cenomanian Glaciation Hypothesis. An alternative scenario that explains both the observed radiogenic and unradiogenic excursions must be examined.

4. 3 The High Arctic Large Igneous Province

The patterns of Os_i variation observed in Iona-1 and in the English Chalk (Jarvis et al., 2017, 2018) are incompatible with a CLIP triggering of the MCE. For Ocean Anoxic Event 2, Turgeon and Creaser (2008) identified, and Du Vivier et al. (2014) later corroborated, an Atlantic-wide unradiogenic Os_i decline to mantle-like values of ~0.2 that predated that event's $\delta^{13}C$ excursion. Because the CLIP was active during this period, multiple workers have proposed that CLIP volcanism, with an associated rise in pCO_2, played a role in triggering OAE-2 (i.e. Snow et al., 2005). However, the connection between OAE-2 and CLIP magmatism has never been conclusively proven, largely because published ages of known CLIP basalts of 98.7 Ma (Serrano et al., 2011), 99.2 Ma and 90.6 Ma (Spikings et al., 2014 and reference therein) do not correlate with OAE-2 (96.4 to 96.5 Ma).

As such, the eruption of the High Arctic Large Igneous Province has been proposed as an alternative triggering mechanism for both OAE-2 and the MCE (i.e. Eldrett et al., 2014). Because of the CLIP's proximity to Iona-1 (figure 1) and the prevailing pattern of northward flow of Atlantic-Tethyan water into the KWIS during the mid-Cenomanian (Eldrett et al., 2015b), any influx of CLIP-derived unradiogenic Os during the MCe would have appeared early in the Iona-1 Os_i reconstruction, as during OAE-2, and resulted in mantle-like Os_i values of ~0.2. Alternatively, a HALIP eruption at the onset of the MCE would not have necessarily resulted in an immediate unradiogenic Os_i excursion, because at the time of the MCE, Iona-1 was isolated from the Arctic

Ocean (figure 1) and therefore any unradiogenic Os input would have had to circuitously travel through the Norwegian Seaway and the Atlantic Ocean before reaching the southern KWIS. This process would have delayed the arrival of a HALIP Os-isotope excursion and may have possibly diluted the expected unradiogneic Os_i signal as well.

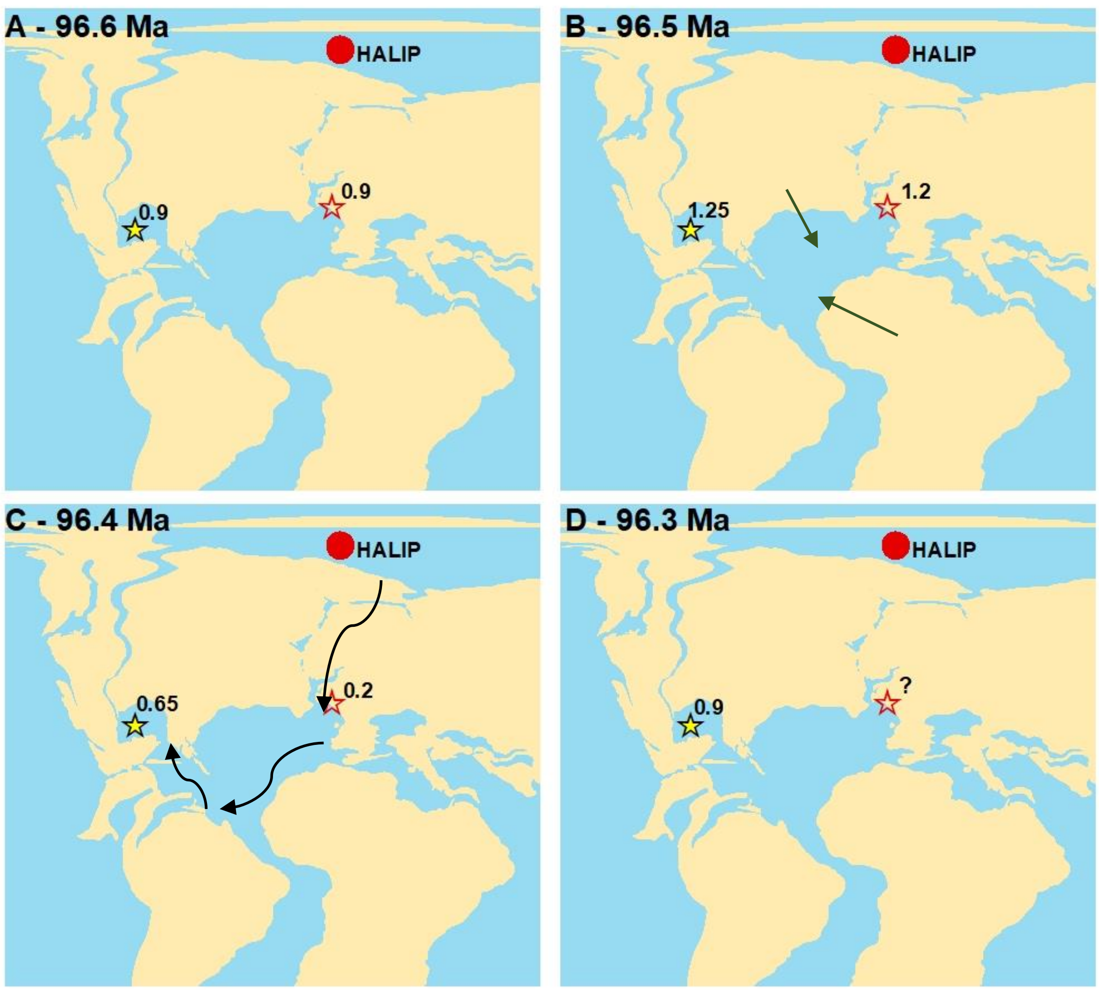

Figure 4: A proposed sequence of seawater Os_i during for the Mid-Cenomanian is shown in the above maps. The location of the High Arctic Large Igneous Province is indicated by the red circle. The Iona-1 Os_i values are represented by the yellow stars

and the adjacent numbers. The Eastbourne Os_i values of Jarvis et al. (2017, 2018) correspond with the hollow red stars

Support for a HALIP-triggering hypothesis comes from published ages of HALIP basalts that coincide with the MCE (Estrada, 2015) and a comparison of the Iona-1 Os_i record with those of the Eastbourne Chalk (Jarvis et al., 2017, 2018). Estrada (2015) reports a composite ^{40}Ar-^{39}Ar age of basalts from Ellesmere Island, Canada, of 96.4 ± 1.4 Ma. Remarkably, the unradiogenic Os_i minimum of 0.65 in Iona-1 in segment C, which could be interpreted as an input of unradiogenic Os from a LIP eruption, occurs at exactly 96.4 Ma (figure 2). Jarvis et al. (2017) similarly notes an unradiogenic $^{187}Os/^{188}Os$ excursion at Eastbourne, England (figure 4), on the order of that seen for OAE-2 (Turgeon and Creaser, 2008), above the MCE double-peak $\delta^{13}C$ excursion. Although the Os_i of seawater has long been considered to be largely homogenous throughout the global ocean on time scales of 10s kyr (Peucker-Ehrenbrink, 2000), more recent investigations have found that paleoseawater $^{187}Os/^{188}Os$ was at times heterogeneous on scales of as little as a few hundred kilometers (Rooney et al., 2016), which would imply a markedly shorter Os residence time. Notably, Cohen and Coe (2006) found that the influx of unradiogenic Os to seawater caused by the eruption of the Central Atlantic Magmatism Province (CAMP) during the Jurassic resulted in a heterogeneous Os_i response, with sites proximal to the CAMP displaying markedly lower Os_i than distal locations.

With these lines of evidence, the following chronology for the Mid-Cenomanian Event is proposed here (figures 2 and 4). Before the onset of the MCE at 96.6 Ma, during segment A in Iona-1, Os_i was stable at approximately 0.9. The MCE was triggered by HALIP volcanism, which resulted in an influx of CO_2 to the atmosphere that raised temperatures and accelerated the global hydrologic cycle. The radiogenic Os_i excursion seen at 96.5 Main segment B of Iona-1 and in the Eastbourne section record the consequent increased continental weathering rates.

As noted above, an investigation of clay mineral assemblages in the Aquitaine Basin, France, confirms this interval of the MCE was warm and humid (Andrieu et al., 2015), which is consistent with this scenario. A similar weathering response is known for OAE-2 (Blätter et al., 2011; Poulton et al., 2015). At the Cenomanian-Turonian boundary, the connection between the Arctic Ocean and Atlantic Ocean through the KWIS was fully established (Minisini et al., 2018), which allowed for efficient and rapid mixing of their waters and consequently their Os_i signals. Therefore, during OAE-2 the unradiogenic Os sourced from the HALIP appeared in Iona-1 immediately at approximately 96.5 Ma, and any increased radiogenic inputs were masked by the mass balance of a greater increase in mantle-derived Os. Conversely, because the southern KWIS was isolated from the Arctic Ocean throughout the MCE-interval, the expected unradiogenic Os_i excursion was delayed in reaching Iona-1 by up to 150 kyr. In the time of segment C, HALIP activity continued, and the unradiogenic Os_i signal entered the Atlantic Ocean through the open Norwegian Seaway.

Seawater εNd reconstructions and paleontological investigations of the English Chalk confirm that several pulses of northerly boreal seawater moved into the North Atlantic during the MCE (Zheng et al., 2013, 2016). The larger magnitude of the Eastbourne Os_i minimum than that of Iona-1 supports a northerly Os source. By the time the HALIP-sourced Os reached Iona-1 in segment C at 96.4 Ma, the unradiogenic signal had been muted because as the unradiogenic Os-enriched body of water moved southward towards the equator, the unradiogenic Os was removed from solution and the body of water mixed with more radiogenic-rich water masses that altered the original LIP Os signature.

A southward-trending gradient of increased Os_i would therefore have been expected in the Atlantic Ocean during the MCE. This scenario is similar to the heterogeneous Os_i response to CAMP volcanism in the Jurassic reported by Cohen et al. (2006). A volcanic origin for the unradiogenic Os_i excursion of interval C is supported by a contemporaneous spike in Hg and Hg/TOC in Iona-1 (figure 2), which began immediately after the radiogenic maximum of interval B at 96.48 Ma and peaked coevally with the Os_i minimum of interval C at 96.39 Ma (Scaife et al., 2017). Though Scaife et al. (2017) proposed CLIP activity as the source of the observed Hg enrichment during the MCe, they also noted that a HALIP origin was possible, depending on future correlations of LIP and OAE ages. Following the MCE's cessation, Os_i returned to background values of ~0.9 in segment D.

Lastly, the evidence presented here sheds new light onto OAE-2 and its relationship to the MCE. The new Os data for the Iona-1 core through the MCE and the similarities between the two events are consistent with the triggering mechanism for both events being HALIP magmatism as proposed in the scenario above. For OAE-2, this conclusion is supported by the recognition of increasing enrichments of mafic trace metals in the KWIS from south to north (Eldrett et al., 2014). The comparisons of Os-isotope data from Iona-1 and Eastbourne presented above confirm a northerly source of volcanic activity, which imparted seawater with identifying Os_i and Hg signatures that then migrated southward and laterally via ocean transport. Ultimately, then, the initiation mechanism for both the Mid-Cenomanian Event and Ocean Anoxic 2, during the Earth's warmest interval in the past 200 Ma (Vezier et al., 1999), was the emplacement of the High Arctic Large Igneous Province, not the Caribbean Large Igneous Province.

5. CONCLUSIONS

Here, the first reconstruction of mid-Cenomanian seawater $^{187}Os/^{188}Os$ in the Cretaceous Western Interior Seaway is presented. These new data $^{187}Os/^{188}Os$ data are not consistent with the Mid-Cenomanian Glaciation Hypothesis. Contrary to the expected Os-isotope response for this hypothesis, the observed $^{187}Os/^{188}Os$ minimum does not correspond with a sea-level fall that would have occurred had substantial covering of the continents had reduced radiogenic Os input to the ocean. Rather, the MCE interval features both radiogenic and unradiogenic $^{187}Os/^{188}Os$ excursions, which can be correlated across the Atlantic. A comparison of these findings to earlier investigations of the Hg and Os-isotope records of the MCE are consistent with a scenario in which High Arctic Large Igneous Province magmatism may have triggered the event. The OAE-2 may have also been initiated by High Arctic Large Igneous Province activity. These new data serve as a benchmark for future Re-Os studies of the MCE.

REFERENCES CITED

Andrieu, S., Brigaud, B., Rabourg, T., and Noret, A., 2015, The Mid-Cenomanian Event in shallow marine environments; Influence on carbonate producers and depositional sequences (northern Aquitaine Basin, France): Cretaceous Research, v. 56, p. 587-607, doi:10.1016/j.cretres.2015.06.018.

Becker, H., Horan, M.F., Walker, R.J., Gao, S., Lorand, J.-P., and Rudnick, R.L., 2006, Highly siderophile element composition from new data on peridotite massifs and xenoliths; Geochemica et Cosmochimica Acta, v. 70, p. 4528-4550, doi:10.1016/j.gca.2006.06.004.

Birck J.-L., Roy-Barman M. and Capmas F. (1997) Re–Os isotopic measurements at the femtomole level in natural samples: Geostandards Newsletter, v. 20, p. 19–27.

Blätter, C.L., Jenkyns, H.C., Reynard, L.M., and Henderson, G.M., 2011, Significant increases in global weathering during Oceanic Anoxic Events 1a and 2 indicated by calcium isotopes: Earth and Planetary Science Letters, v. 309, p. 77-88, doi:10.1016/j.espi2011.06.029.

Bottini, C., Cohen, A., Erba, E., Jenkyns, H., and Coe, A., 2012, Osmium-isotope evidence for volcanism, weathering, and ocean mixing during the early Aptian OAE 1a; Geology, v. 40, p. 583-586, doi:10.1130/G33140.1.

Coccioni, R., and Galeotti, S., 2003, The mid-Cenomanian Event: prelude to OAE 2: Palaeogeography, Palaeoclimatology, Palaeoecology, v. 190, p. 427-440, doi:10.1016/S0031-0182(02)00617-X.

Chen, K., Walker, R.J., Rudnick, R.L., Gao, S., Gasching, R.M., Puchtel, I.S., Tang, M., and Hu Z.-C., 2016, Platinum-group element abundances and Re-Os isotopic systematics of the upper continental crust through time: Evidence from glacial diamictites, Geochemica et Cosmochimica Acta, v. 191, p. 1-16, doi:10.1016’j.gca.2016.07/004.

Cohen, A., and Waters, F., 1996, Separation of osmium from geological materials by solvent extraction for analysis by thermal ionization mass spectrometry: Analytica Chimica Acta, v. 332, p. 269-275.

Cohen, A., 2004, The rhenium-osmium isotope system: applications to geochronological and paleoenvironmental problems: Journal of the Geological Society, London, v. 161, p. 729-734.

Cohen, A.S., and Coe, A.L., 2006, The impact of the Central Atlantic Magmatic Province on climate and on the Sr- and Os-isotope evolution of seawater:

Palaeogeography, Palaeoclimatology, Palaeoecology, v. 244, p., 374-390, doi:10.1016/j.palaeo.2006.06.036.

Cohen, A.S., Coe, A.L., Harding, S.M., Scwark, L., 2004, Osmium isotope evidence for the regulation of atmospheric CO_2 regulation by continental weathering: Geology, v. 32, p. 157-160, doi:10.1130/G20158.1.

Deegan, F.M., Troll, V.R., Bedard, J.H., Evenchick, C.A., Dewing, K., Grasby, S., Geiger H., Freda, C., Misiti, V., and Mollo, S., 2016, The stiff upper LIP: investigating the High Arctic Large Igneous Province: Geology Today, v. 32., p. 92-96.

Du Vivier, A., Selby, D., Sageman, B., Jarvis, I., Gröcke, D., and Voigt, S., 2014, Marine $^{187}Os/^{188}Os$ isotope stratigraphy reveals the interaction of volcanism and ocean circulation during Oceanic Anoxic Event 2, Earth and Planetary Science Letters, v. 389, 23-33, doi:10.1016/j.epsl.2013.12.024.

Eldrett, J., Minisini, D., and Bergman, S., 2014, Decoupling of the carbon cycle during Ocean Anoxic Event 2: Geology, v. 42, p. 567-570, doi:10.1130/G35520.1.

Eldrett, J.S., Ma, C., Bergman, S.C., Lutz, B., Gregory, F.J., Dodsworth, P., Phipps, M., Minisini, D., Ozkan, A., Ramezani, J., Bowring, S.A., Kamo, S.L., Ferguson, K., Macaulay, C., and Kelly, A.E., 2015, An astronomically calibrated stratigraphy of the Cenomanian,Turonian and earliest Coniacian from the Cretaceous Western Interior Seaway, USA: Implications for global chronostratigraphy: Cretaceous Research, v. 56, p. 316-344, doi:10.1016/j.cretres.2015.04.010.

Eldrett, J.S., Ma, C., Bergman, S.C., Ozkan, A., Minisini, D., Lutz, b., Jackett, S.J., Macaulay, C., and Kelly, A.E., 2015, Origin of limestone–marlstone cycles: Astronomic forcing oforganic-rich sedimentary rocks from the Cenomanian to early Coniacian of the Cretaceous Western Interior Seaway, USA: Earth and Planetary Science Letters, v. 423, p. 98-113, doi:10.1016,/j.epsl.2015.04.026.

Estrada, S., 2015, Geochemical and Sr–Nd isotope variations within Cretaceous continental flood-basalt suites of the Canadian High Arctic, with a focus on the Hassel Formation basalts ofnortheast Ellesmere Island: International Journal of Earth Science, v.104, p. 1981-2005, doi:10.1007/s00531-014-1066-x.

Friedrich, O., Erbacher, J., and Mutterlose, J., 2006, Paleoenvironmental changes across the Cenomanian/Turonian Boundary Event (Oceanic Anoxic Event 2) as indicated by benthic foraminifera from the Demerara Rise (ODP Leg 207): Revue de Micropaléontologie, v. 49, p. 121–139, doi:10.1016/j.marmicro.2009.01.002.

Friedrich, O., Erbacher, J., Wilson, P., Moriya, K., and Mutterlose, J., 2009, Paleoenvironmental changes across the Mid Cenomanian Event in the tropical

Atlantic Ocean (Demerara Rise, ODP Leg 207) inferred from benthic foraminiferal assemblages: Marine Micropaleontology, v. 71, p. 28-40.

Giraud, F., Reboulet, S., Deconinck, J.F., Martinez, M., Carpentier, A., and Bréziat, C., 2013, The Mid- Cenomanian Event in southeastern France: Evidence from paleontological and clay mineralogical data; Cretaceous Research, v. 46, p. 43-59, doi:10.1016/j.cretres.2013.09.004.

Holmden, C., Jacobson, A.D., Sageman, B.B., and Hurtgen, M.T., 2016, Response of the Cr isotope proxy to Cretaceous Ocean Anoxic Event 2 in a pelagic carbonate section from the Western Interior Seaway: Geochimica et Cosmochimica Acta, v. 186, p. 277-297, doi:10.1016/j.gca.2016.04.039.

Jarvis, I., Sascha, R.-E., and Selby, D., 2017, Mid-Cenomanian Event I (MCE I, 96 Ma): elemental and osmium isotope evidence for sea level, climate, and palaeocirculation changes in the NW European epicontinental sea: European Geosciences Union General Assembly, 19th, Vienna, Austria, p. 3731.

Jarvis, I., Sascha, R.-E., and Selby, D., 2018, Linking sea level, climate, and palaeocirculation change during Mid-Cenomanian Event I (MCE I, 96 Ma): elemental and osmium isotope evidence from southern England: European Geosciences Union General Assembly, 20th, Vienna, Austria, p. 7132.

Jaffe, L.A., Peucker-Ehrenbrink, B., and Petsch, S.T., Mobility of rhenium, platinum group elements and organic carbon during black shale weathering; Earth and Planetary Science Letters, v. 198, p. 339-353, doi:10.1016/S0012-821X(02)005526-5.

Jenkyns, H.C., 2010, Geochemistry of oceanic anoxic events: Geochemistry, Geophysics, Geosystems, v. 11, doi:10.1029/2009GC002688.

Minisinsi, D., Eldrett, J., Bergman, S., and Forkner, R., 2018, Chronostratigraphic framework and depositional environments in the organic-rich , mudstone-dominated Eagle Ford Group, Texas, USA: Sedimentology, doi:10.1111/sed.12437.

Percival, L.M.E., Cohen, A.S., Davies., M.K., Dickson, A.J., Jenkyns, H.C., Leng, N.J., Mather, T.A., Storm, M.S., and Xu, W., 2016, Osmium isotope evidence for two pulses of increased continental weathering linked to Early Jurassic volcanism and climate change: Geology, v. 44, p. 759-762, doi:10.1130/G37997.1.

Peucker-Ehrenbrink, B. and Hannigan, R., 2000, Effects of black shale weathering on the mobility of rhenium and platinum group elements: Geology, v. 28, p. 475-478.

Peucker-Ehrenbrink, B. and Ravizza, G., 2002, The marine osmium isotope record: Terra Nova, v. 12, doi:10.1046/j.1365-3121.2000.00295.x.

Poulton, S.W., Henkel, S., März, C., Urquhart, H., Flögel, S., Kasten, S., Damsté, J.S.S., and Wagner, T., 2015, A continental-weathering control on orbitally driven redox-nutrient cycling during Cretaceous Oceanic Anoxic Event 2: Geology, v. 43, p. 963-966, doi:10.1130/G36837.1.

Rooney, A.D., Selby, D., Lloyd, J.M., Roberts, D.H., Lückge, A., Sageman, B.B., and Prouty, N.G., 2016, Tracking millennial-scale Holocene glacial advance and retreat using osmium isotopes: Insights from the Greenland ice sheet: Quaternary Science Reviews, v. 138, p. 49-61, doi:10.1016/j.quascirev.2016.02.021.

Sawlowicz, S., 1993, Iridium and other platinum-group elements as geochemical markers in sedimentary environments: Palaeogeography, Palaeoclimatology, Palaeoecology, v. 104, p. 253-270.

Scaife, J., Ruhl, M., Dickson, A., Mather, T., Jenkyns, H., Percival, L., Hesselbo, S., Cartwright, J., Eldrett, J., Bergman, S., and Minisini, D., 2017, Sedimentary Mercury Enrichments as a Marker for Large Igneous Province Volcanism: Evidence from the Mid-Cenomanian Event and Ocean Anoxic Event 2 (Late Cretaceous): Geochemistry, Geophysics, Geosystems, v. 18, p. 4253-4275, doi:10.1002/2017GC007153.

Serrano, L., Ferrari, L., Martinez, M.L., Petrone, C.M., and Jaramillo, C., 2011, An integrative geologic, geochronologic and geochemical study of Gorgona Island, Colombia: Implications for the formation of the Caribbean Large Igneous Province: Earth and Planetary Science Letters, v. 309, p. 324 – 336, doi:10.1016/j.epsl.2011.07.011.

Spkings, R., Cochrane, R., Villagomez, D., Van der Lelij, R., Vallejo, C., Winkler, W., and Beate, B., 2014, The geological history of northwestern South America: from Pangaea to the early collision of the Caribbean Large Igneous Province (290–75 Ma): Gondwana Research, v. 27, p. 95-139, doi: 10.1016/j.gr.2014.06.004.

Turgeon, S., and Creaser, R., 2008, Cretaceous oceanic anoxic event 2 triggered by a massive magmatic episode: Nature, v. 454 , p. 323-326, doi:10.1038/nature07076.

Vezier, J., Davin, A., Karem, A., Bruckschen, P., Buhl., D., Bruhn., F., Carden G.A.F., Diener, A., Ebneth, S., Godderis, Y., Jasper, T., Korte, C., Pawellek, F., Podlaha, O.G., and Straus, H., 1999, $^{87}Sr/^{86}Sr$, $\delta^{13}C$ and $\delta^{18}O$ evolution of Phanerozoic seawater: Chemical Geology, v. 161., p. 59-88.

Zheng, X-Y., Jenkyns, H.C., Gale, A.S., Ward, D.J., and Henderson, G.M., 2013, Changing ocean circulation and hydrothermal inputs during Ocean Anoxic Event 2 (Cenomanian-Turonian): Evidence from Nd-isotopes in the European shelf sea

Zheng, X-Y., Jenkyns, H.C., Gale, A.S., Ward, D.J., and Henderson, G.M., 2016, A climatic control on reorganization of ocean circulation during themid-Cenomanian event and Cenomanian-Turonian oceanic anoxic event (OAE 2): Nd isotope evidence: Geology, v. 44, p. 151-154, doi:10.1130/G37354.1.